

Supplementary Materials

Advancing CO₂ conversion: integrated use of dual active catalytic sites in flexible, porous polymeric porphyrin and ionic liquid composite networks

Liping Zheng¹, Can Fang¹, Zhenghai Chen², Jingxu Han¹, Zhouxian Wang¹, Tonghao Dai¹, Jiacong Ma¹, Zhifeng Dai^{1,3,*}, Yubing Xiong^{1,3,*}, Qi Sun^{4,*}

¹Key Laboratory of Surface & Interface Science of Polymer Materials of Zhejiang Province, School of Chemistry and Chemical Engineering, Zhejiang Sci-Tech University, Hangzhou 310018, Zhejiang, China.

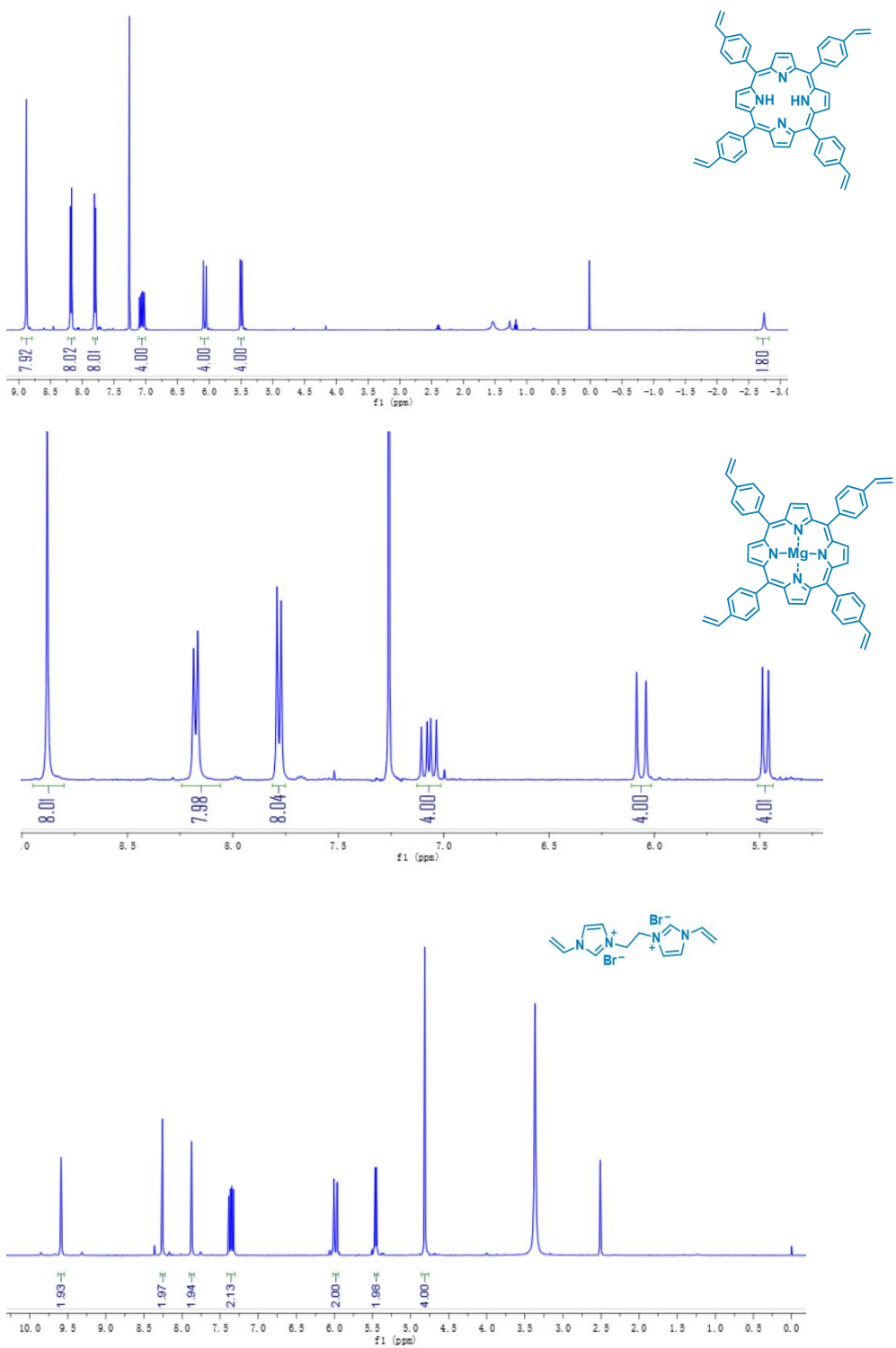
²Kente Catalysts Inc., Taizhou 317306, Zhejiang, China.

³Zhejiang Sci-Tech University, Shengzhou Innovation Research Institute, Shengzhou 312400, Zhejiang, China.

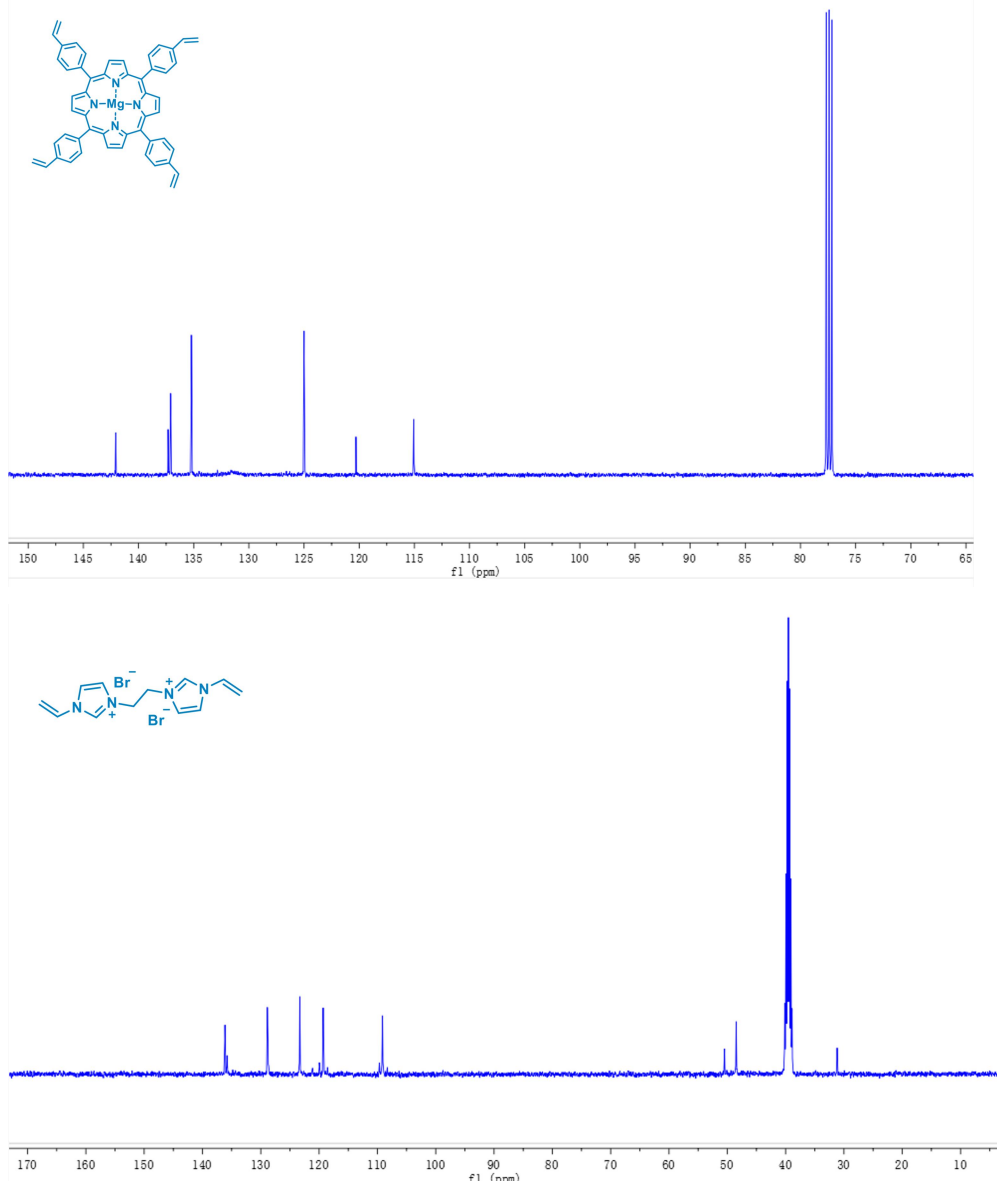
⁴Zhejiang Provincial Key Laboratory of Advanced Chemical Engineering Manufacture Technology, College of Chemical and Biological Engineering, Zhejiang University, Hangzhou, 310027, Zhejiang, China.

***Correspondence to:** Prof. Qi Sun, Zhejiang Provincial Key Laboratory of Advanced Chemical Engineering Manufacture Technology, College of Chemical and Biological Engineering, Zhejiang University, Hangzhou 310027, Zhejiang, China.

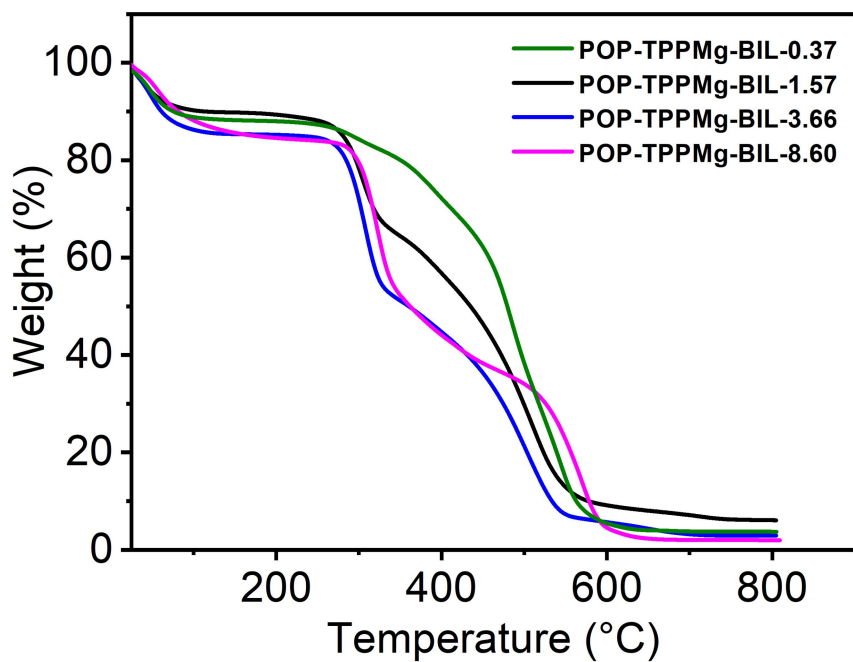
E-mail: sunqichs@zju.edu.cn; Prof. Yubing Xiong, Dr. Zhifeng Dai, Key Laboratory of Surface & Interface Science of Polymer Materials of Zhejiang Province, School of Chemistry and Chemical Engineering, Zhejiang Sci-Tech University, Hangzhou 310018, Zhejiang, China. E-mail: yubing_xiong@163.com; daizhifeng1988@163.com



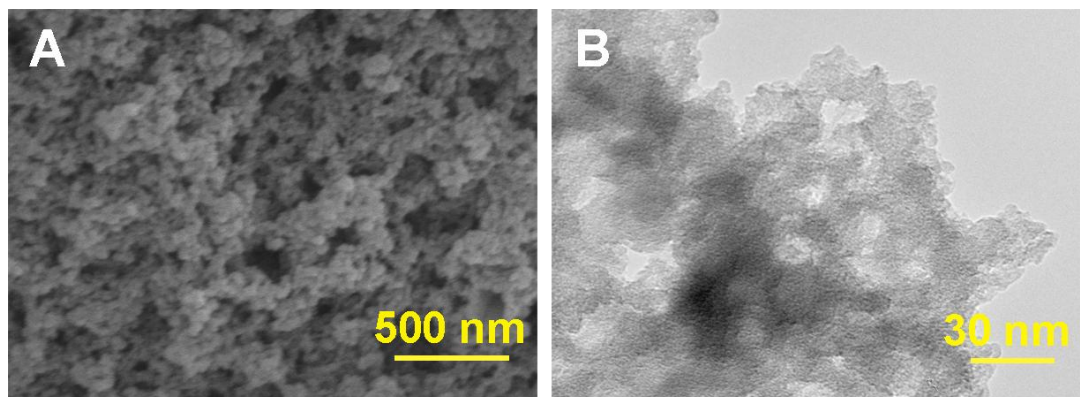
Supplementary Figure 1. ^1H NMR spectra of v-TPP, v-TPPMg, and BIL.



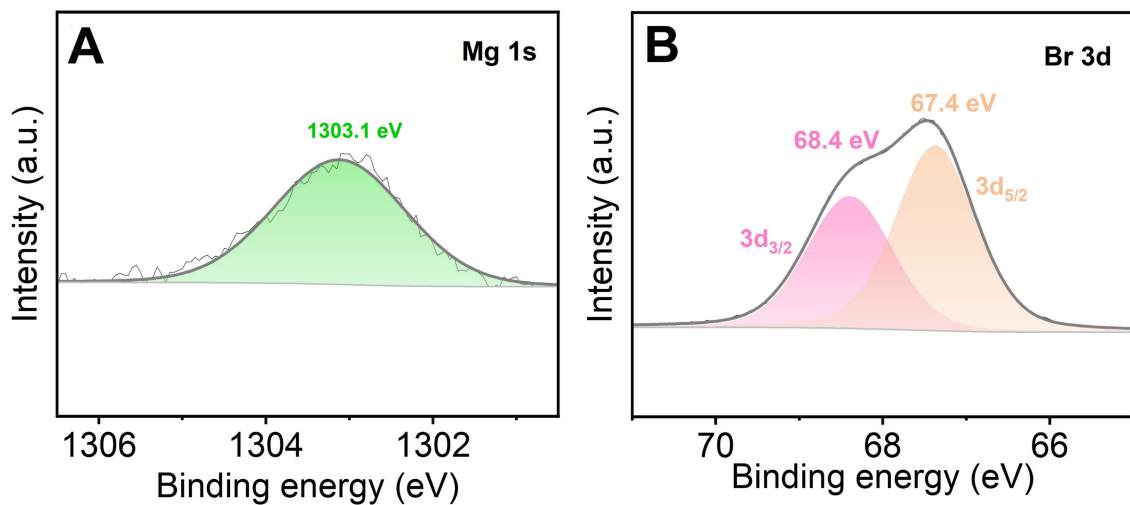
Supplementary Figure 2. ${}^{13}\text{C}$ NMR spectra of v-TPPMg and BIL.



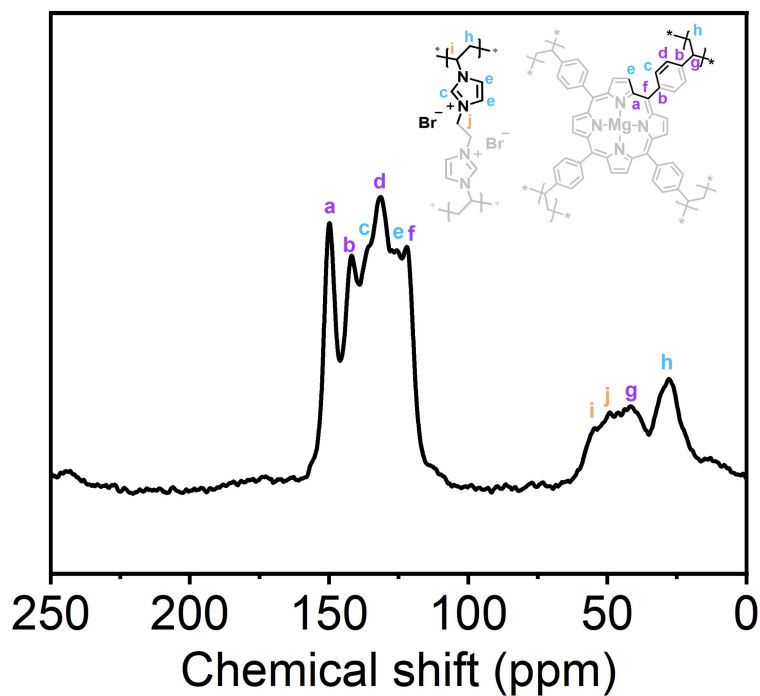
Supplementary Figure 3. TG curves of POP-TPPMg-BIL-x.



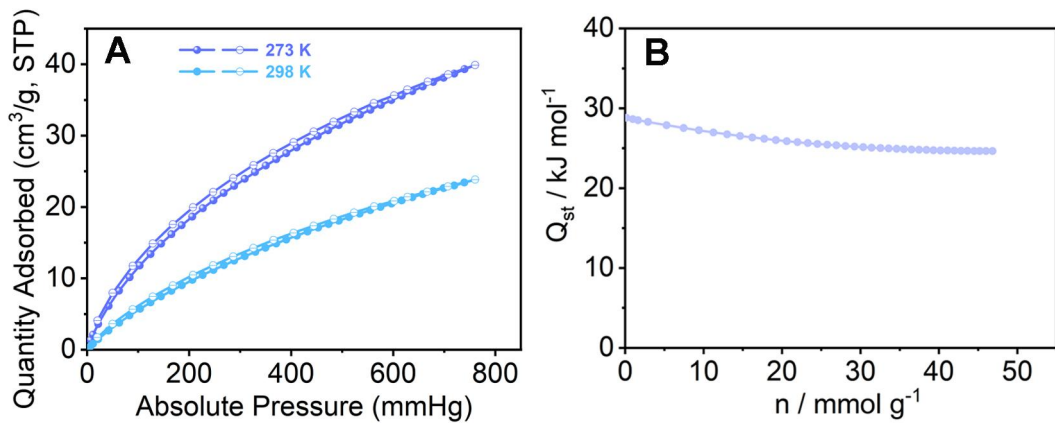
Supplementary Figure 4. (A) SEM and (B) high-resolution TEM images of POP-TPPMg.



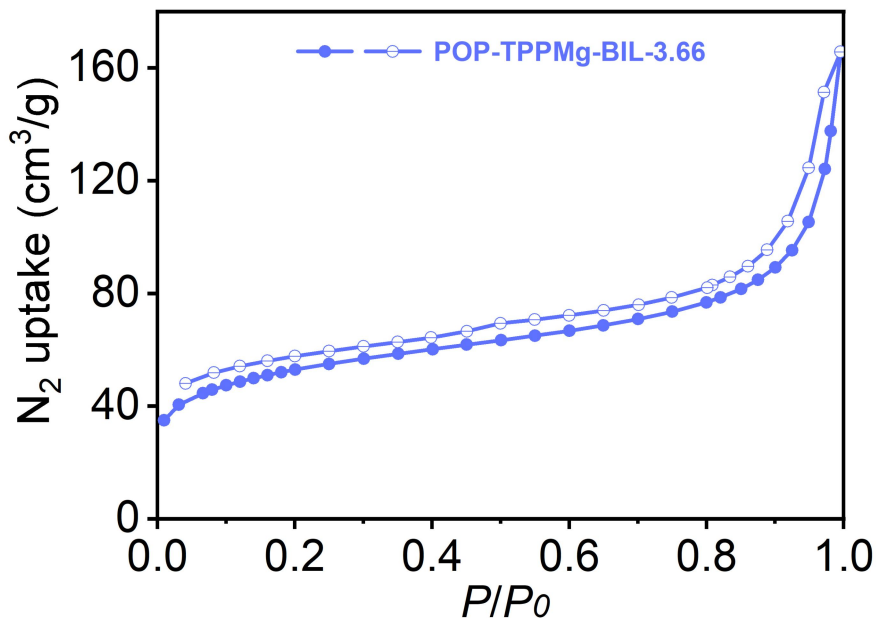
Supplementary Figure 5. (A) Mg 1s, and (B) Br 3d spectra of the as synthesized POP-TPPMg-BIL-1.57 catalyst.



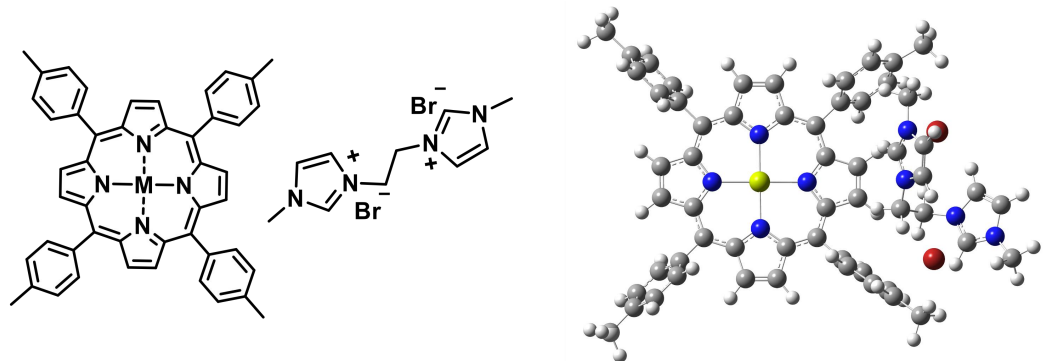
Supplementary Figure 6. ¹³C MAS NMR spectrum of POP-TPPMg-BIL-1.57.



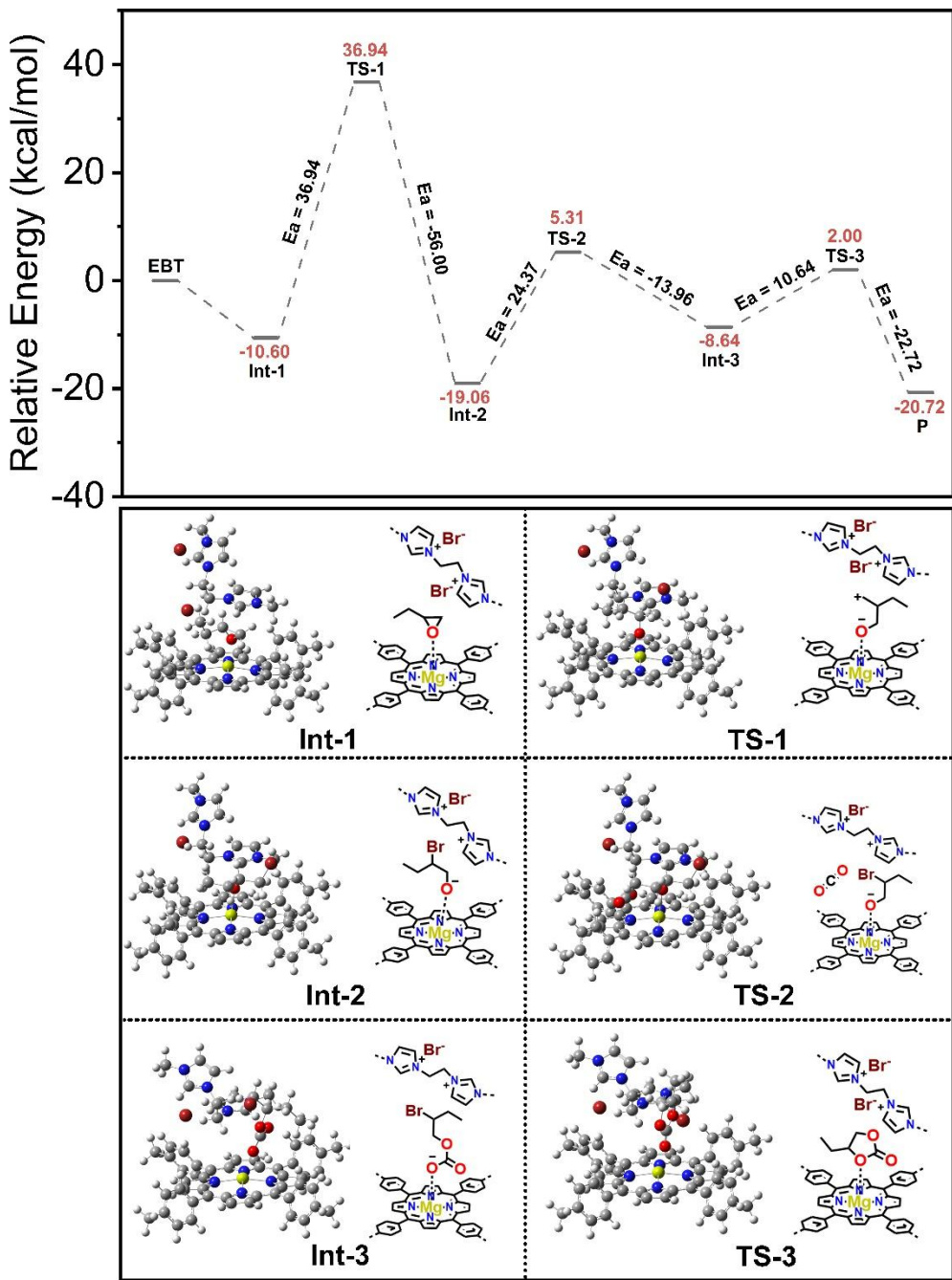
Supplementary Figure 7. (A) CO₂ sorption isotherms at different temperatures for POP-TPPMg-BIL-1.57 and (B) the calculated isosteric heat (Q_{st}) by Virial Method.



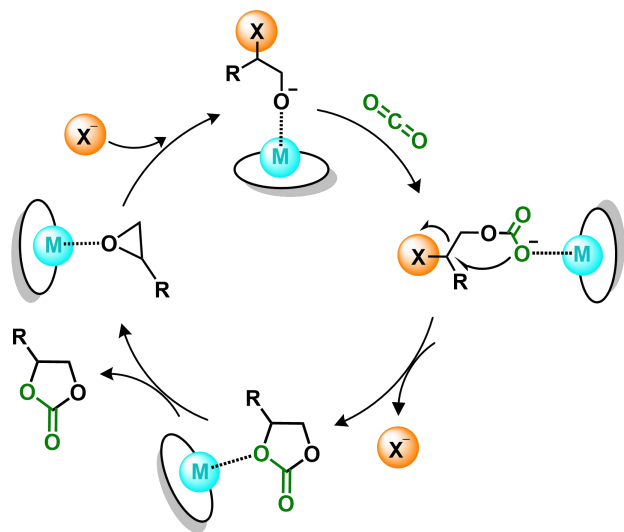
Supplementary Figure 8. N₂ sorption isotherms for POP-TPPMg-BIL-3.66. The BET surface area and pore volume were calculated to be 174 m²/g and 0.26 cm³/g, respectively.



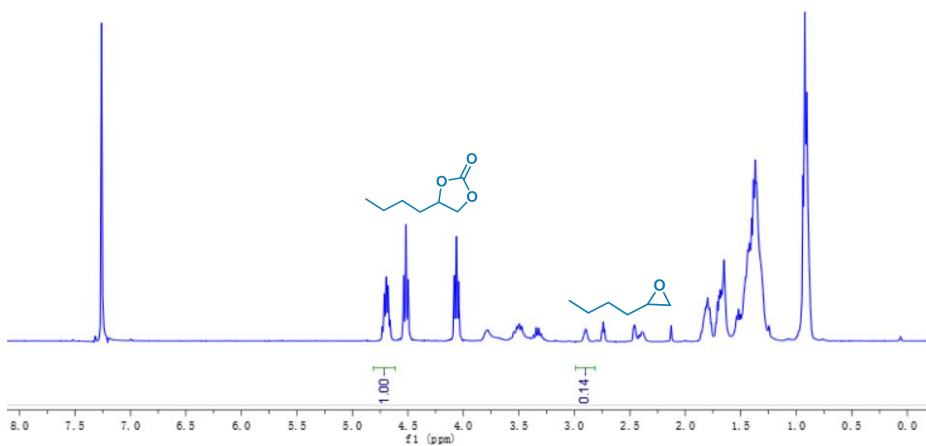
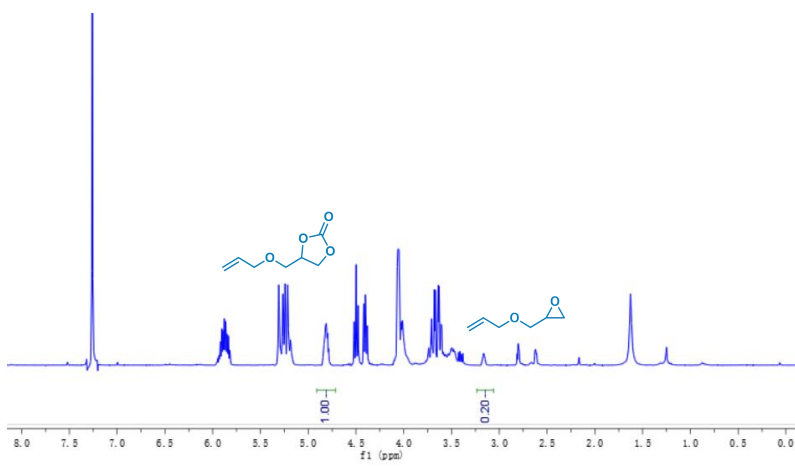
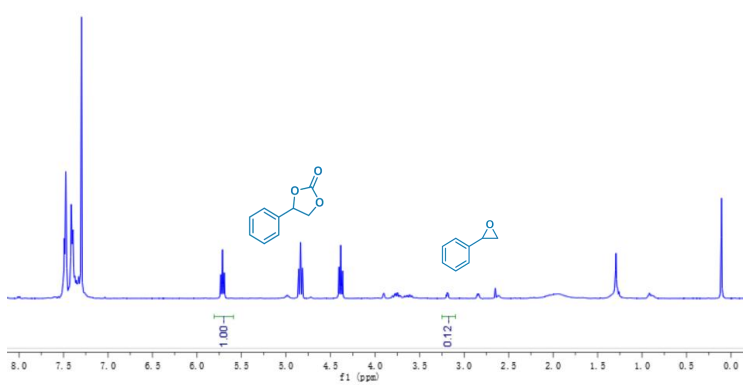
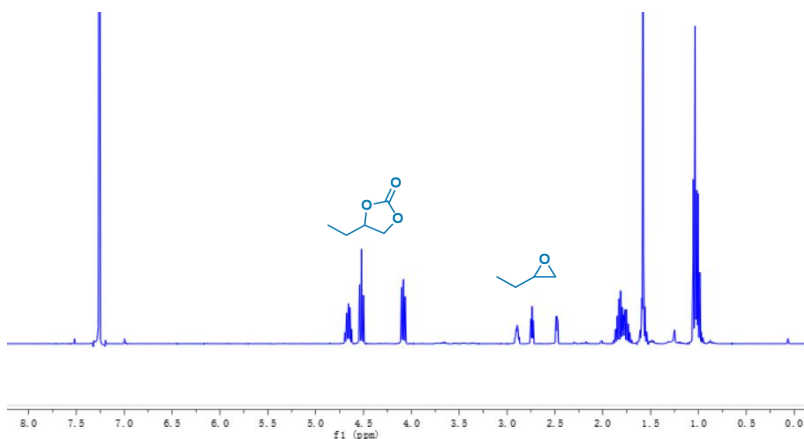
Supplementary Figure 9. For simplicity in the calculations, the structure of POP-TPPMg-BIL-1.57 is represented by the simplified structures shown (white: H, gray: C, blue: N, yellow: Mg, red: Br).

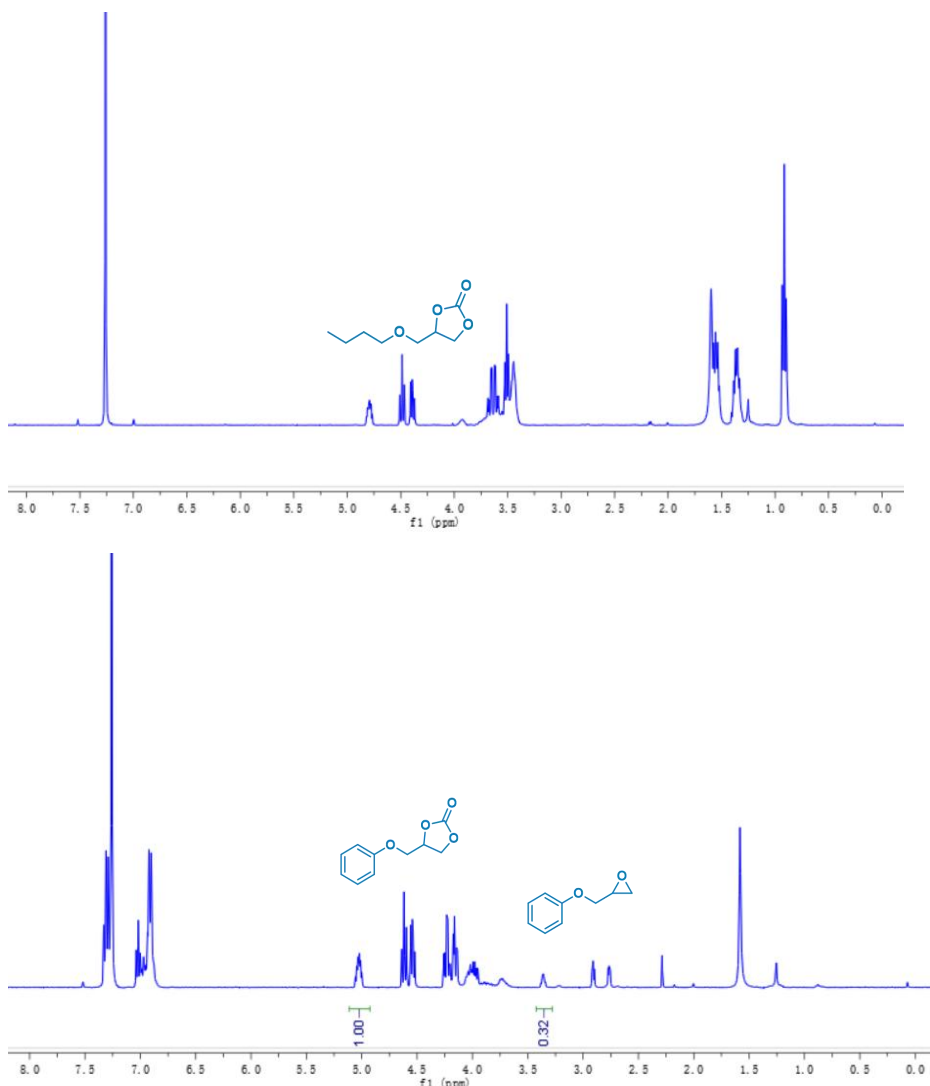


Supplementary Figure 10. DFT-calculated free energy profiles and the optimized geometries of key intermediates and transition states for the POP-TPPMg-BIL-1.57 catalyzed CO₂ cycloaddition with 1,2-epoxybutane (white: H, gray: C, blue: N, yellow: Mg, red: Br).

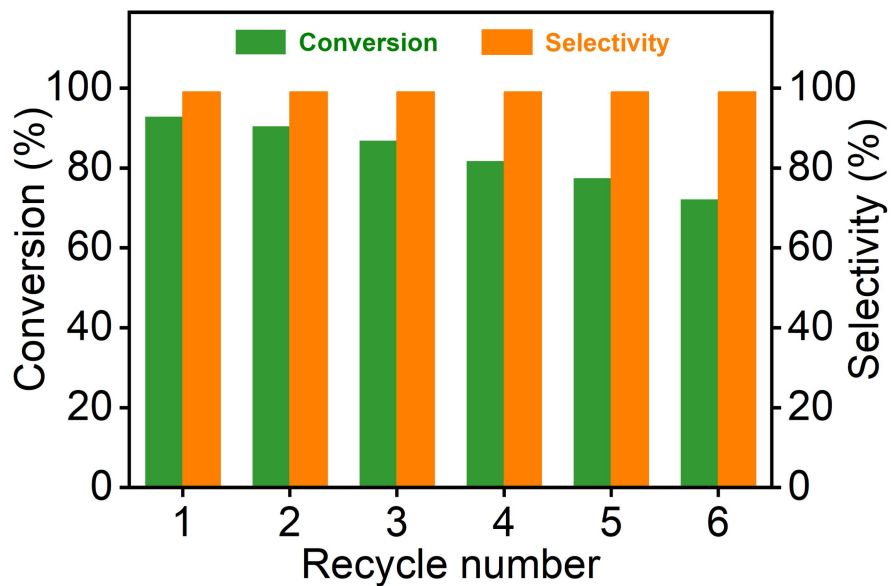


Supplementary Figure 11. Proposed mechanism of cycloaddition between CO_2 and epoxides over bifunctional heterogeneous catalysts.

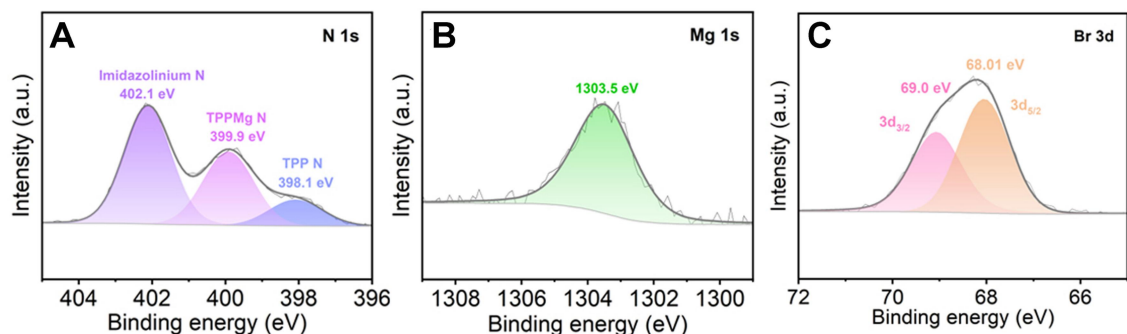




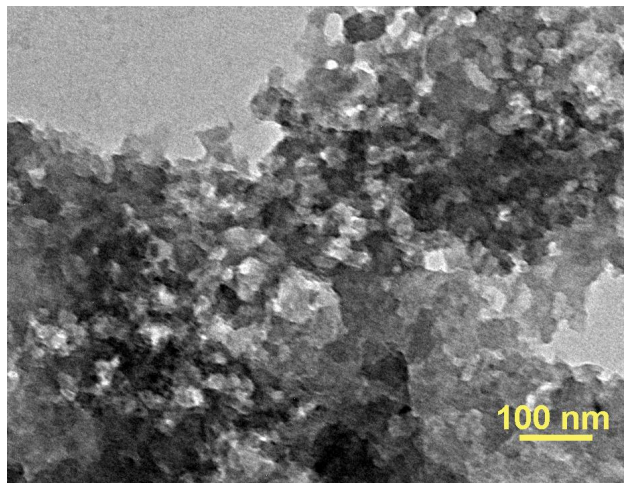
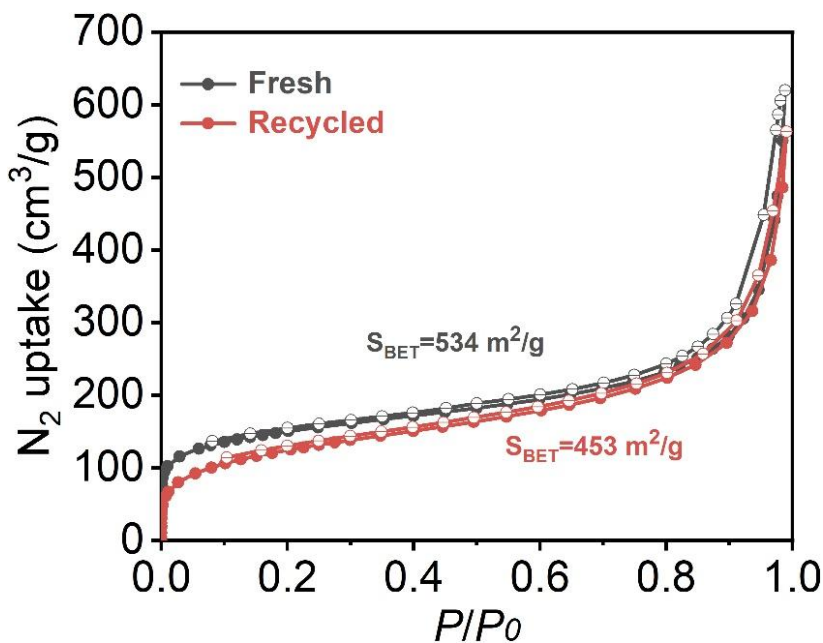
Supplementary Figure 12. ¹H NMR spectra of various products.



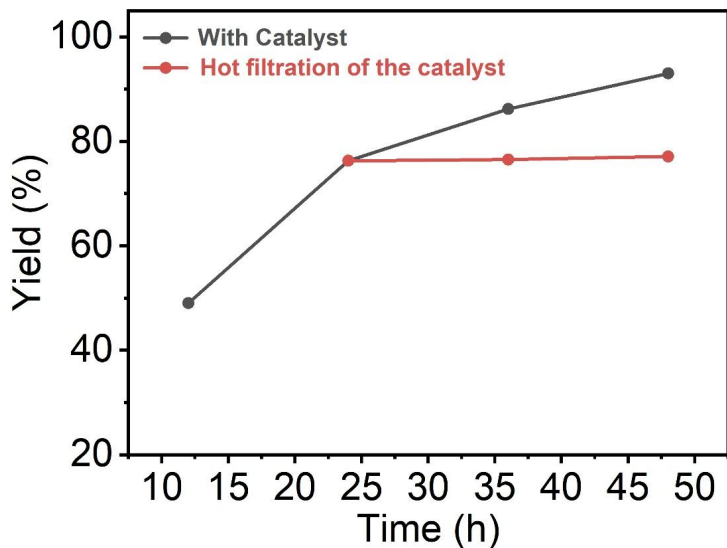
Supplementary Figure 13. Conversion and selectivity during recycling tests in the cycloaddition of 1,2-epoxybutane with CO₂ using the POP-TPPMg-BIL-1.57 catalyst. Reaction conditions: 1,2-epoxybutane (10 mmol), POP-TPPMg-BIL-1.57 (44.4 mg), 50 °C, and 1 atm CO₂.



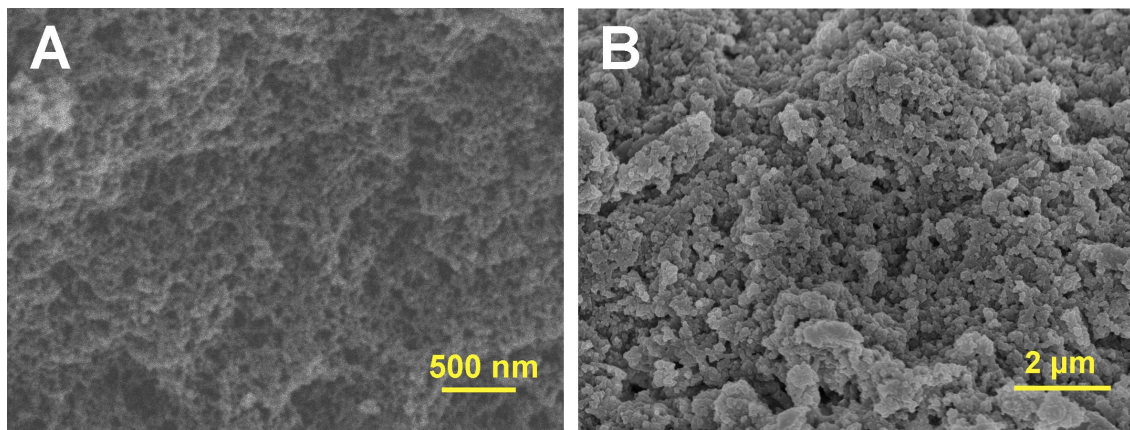
Supplementary Figure 14. (A) N 1s spectrum, (B) Mg 1s spectrum, and (C) Br 3d spectrum of the POP-TPPMg-BIL-1.57 catalyst after six recycling cycles.



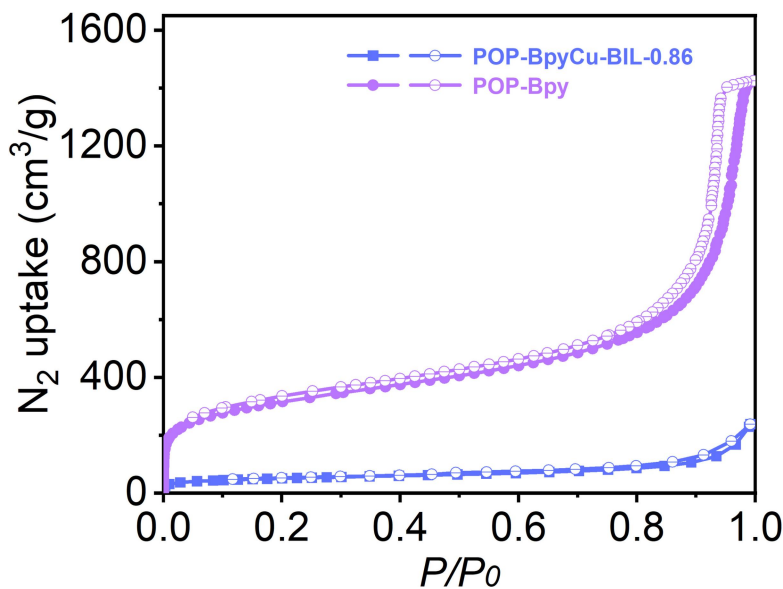
Supplementary Figure 16. TEM image of POP-TPPMg-BIL-1.57 after six recycling cycles.



Supplementary Figure 17. Yield versus reaction time for the cycloaddition reaction between 1,2-epoxybutane and CO₂. Reaction conditions: 1,2-epoxybutane (10 mmol), POP-TPPMg-BIL-1.57 catalyst (44.4 mg), and CO₂ (1 atm) at 50 °C. After 24 hours of reaction, the catalyst was removed via filtration, and the reaction mixture was allowed to proceed for an additional 24 hours. Yields were determined by ¹H NMR spectroscopy.



Supplementary Figure 18. SEM images of (A) POP-Bpy and (B) POP-BpyCu-BIL-0.86.



Supplementary Figure 19. N₂ sorption isotherms of POP-Bpy and POP-BpyCu-BIL-0.86 collected at 77 K. The BET surface areas and pore volumes were calculated as follows: 1123 m²/g and 2.14 cm³/g for POP-Bpy, and 182 m²/g and 0.36 cm³/g for POP-BpyCu-BIL-0.86.

Supplementary Table 1. Comparison of catalytic performance between POP-TPPMg-BIL-1.57, TPPMg&BIL, and the POP-TPPMg&BIL binary system in the cycloaddition of CO₂ with 1,2-epoxybutane^a.

Entry	Catalyst	Time (h)	Conv. (%) ^b
1	POP-TPPMg-BIL-1.57	48	99
2	BIL/TPPMg	48	99
3	BIL/POP-TPPMg	48	95

^aReaction conditions: 1,2-epoxybutane (10 mmol), POP-TPPMg-BIL-1.57 catalyst (44.4 mg, 0.333 mol% and 1.046 mol% based on Mg and Br species, respectively), and CO₂ (1 atm). ^bProduct yield determined by ¹H NMR spectroscopy.

Supplementary Table 2. Comparison of the catalytic performance of this study with other catalytic systems from literature in the cycloaddition of CO₂ with 1,2-epoxybutane.

Entry	Catalyst	T (°C)	Time (h)	Conv. (%)	Ref.
1	POP-TPPMg-BIL-1.57	50	48	89.0	This work
2	POP-PA-NH ₂	60	48	69.4	Ref. S1
3	POP-PA-COOH	60	48	53.6	Ref. S1
4	POP-PA-OH	60	48	54.6	Ref. S1
5	POP-BnCl-CP	60	48	90.1	Ref. S2
6	POP-BnCl-PB	60	48	70.9	Ref. S2
7	POP-BnCl-PP	60	48	61	Ref. S2
8	POP-PBnCl-TPPMg-4	40	48	52.4	Ref. S3
9	POP-PBnCl-TPPMg-12	40	48	89.3	Ref. S3
10	PCP-Cl	100	12	98	Ref. S4
11	Al-iPOP-1	40	6	99	Ref. S5
12	POF-PNA-Br	40	48	98	Ref. S6
13	pPI-1/pPI-2	80	72	98/90	Ref. S7
14	HIP-COOH-TMG	110	8	99	Ref. S8
15	AC-IL-NTf ₂	120	13	83	Ref. S9
16	IP 1	70	6	99.9	Ref. S10
17	IP 2	70	6	85.4	Ref. S10
18	IP 3	70	6	74.6	Ref. S10
19	P-DBTMGH	100	4	96	Ref. S11
20	CoPor-HIP	80	6	96	Ref. S12

Supplementary Table 3. Comparison of catalytic performances across different catalytic systems in the cycloaddition of CO₂ with 1,2-epoxybutane^a.

Entry	Catalyst	Time (h)	Conv. (%) ^b
1	POP-BpyCu-BIL-0.86	48	70.4
2	v-BpyCu&PBIL	48	99.0
3	v-BpyCu&v-BIL	36	99.0
4	POP-BpyCu&PBIL	48	44.8
5	POP-BpyCu-BIL-0.14	48	43.5

^aReaction conditions: 1,2-epoxybutane (1.08 g, 15 mmol), POP-BpyCu-BIL-0.86 catalyst (24.6 mg, corresponding to 0.067 mol% Cu and 0.115 mol% Br based on catalyst content), CO₂ (1 atm), and 50 °C. ^bProduct yield determined by ¹H NMR.

Supplementary References

- [1] Dai Z, Bao Y, Yuan J, Yao J, Xiong Y. Different functional groups modified porous organic polymers used for low concentration CO₂ fixation. *Chem Commun* 2021;57:9732.[DOI: 10.1039/d1cc03178c]
- [2] Bao Y, Liu J, Zhang Y, Zheng L, Ma J, Zhang F, Xiong Y, Meng X, Dai Z, Xiao F-S. Porous organic polymers with diverse quaternary phosphonium units for chemical fixation of CO₂ with low concentration. *Fuel* 2023;331:125909.[DOI: 10.1016/j.fuel.2022.125909]
- [3] Dai Z, Tang Y, Zhang F, Xiong Y, Wang S, Sun Q, Wang L, Meng X, Zhao L, Xiao F-S. Combination of binary active sites into heterogeneous porous polymer catalysts for efficient transformation of CO₂ under mild conditions. *Chin J Catal* 2021;42:618.[DOI: 10.1016/S1872-2067(20)63679-8]
- [4] Buyukcakir O, Je SH, Choi DS, Talapaneni SN, Seo Y, Jung Y, Polychronopoulou K, Coskun A. Porous cationic polymers: the impact of counteranions and charges on CO₂ capture and conversion. *Chem Commun* 2016;52:934-937.[DOI: 10.1039/c5cc08132g]
- [5] Chen Y, Luo R, Xu Q, Jiang J, Zhou X, Ji H. Charged metalloporphyrin polymers for cooperative synthesis of cyclic carbonates from CO₂ under ambient conditions. *ChemSusChem* 2017;10:2534.[DOI: 10.1002/cssc.201700536]
- [6] Ma D, Liu K, Li J, Shi Z. Bifunctional metal-free porous organic framework heterogeneous catalyst for efficient CO₂ conversion under mild and cocatalyst-free conditions. *ACS Sustain Chem Eng* 2018;6:15050.[DOI: 10.1021/acssuschemeng.8b03517]
- [7] Narzary BB, Karatayeva U, Mintah J, Villeda-Hernandez M, Faul CFJ. Bifunctional metal-free porous polyimide networks for CO₂ capture and conversion. *Mater Chem Front* 2023;7:4473.[DOI: 10.1039/D3QM00639E]
- [8] Li M, Shi L, Liu Y, Li S, Cui W, Li W, Zhi Y, Shan S, Miao Y. A dual-ionic hyper-crosslinked polymer for efficient CO₂ fixation and conversion. *Chem Eng J* 2024;481:148550.[DOI: 10.1016/j.cej.2024.148550]
- [9] Alla SC, Prasad D, Kusuma S, Samal AK, Chaudhari NK, Seo JG, Jadhav AH. Engineered ionic liquids supported on activated carbon as a sustainable and selective catalyst for viable fixation of CO₂ into valuable chemicals. *Chem Eng J* 2024;481:148239.[DOI: 10.1016/j.cej.2023.148239]
- [10] Zhu L, Cheng P, Xiao Z, Lu C, Li B, Jiang X, Shen Z, Qian N, Zhong W, He Y,

- Incorporation of phenolic skeleton into imidazolium ionic polymers as recyclable catalysts for efficient fixation of CO₂ into cyclic carbonates. *Chem Eng J* 2024;481:148359.[DOI: 10.1016/j.cej.2023.148359]
- [11]Qu Q, Cheng L, Wang P, Fang C, Li H, Ding J, Wan H, Guan G. Guanidine-functionalized basic binuclear poly(ionic liquid)s for low partial pressure CO₂ fixation into cyclic carbonate. *Sep Purif Technol* 2024;339:126682.[DOI: 10.1016/j.seppur.2024.126682]
- [12]Xu W, Zhang Z, Wu Y, Chen K, Luo R, Cobalt porphyrin-based hypercrosslinked ionic polymers as biomimetic nanoreactors for CO₂ conversion to cyclic carbonates. *Chem Commun* 2024;60:1599.[DOI: 10.1039/D3CC05593K]